Multiphoton Ionization and Fragmentation Process of Benzene at 193 nm Involving Ionization of Neutral Fragments

Yoshihiro MORI* and Taiji KITAGAWA
Department of Pharmaceutical Sciences, Toyama Medical and Pharmaceutical University, Sugitani, Toyama 930-01
(Received November 4, 1992)

Laser flux dependences of multiphoton ionization (MPI) of benzene and benzene-d_6 were measured both in gaseous phase and in molecular beam with ArF (193 nm) and KrF (248 nm) excimer lasers. Several different behaviors were observed at 193 nm in comparison with the MPI at 248 nm: An unexpected enhancement of the MPI efficiency at high laser power involving three-photon ionization process, an unusually small ratio of $(C_4D_4^{+\cdot}+C_4D_3^{+}+C_4D_2^{+\cdot})/C_3D_3^{+}$ (1—2) compared with the ratio expected from the breakdown diagram (3—5) and a very large isotope effect on the relative intensity of $C_4H_4^{+\cdot}/C_4D_4^{+\cdot}$ (0.65). To interpret these phenomena, we propose a new MPI and fragmentation scheme at 193 nm involving two-photon ionization of benzene via the intermediate triplet state(s), possibly T_1 and/or T_2, and one-photon ionization of C_3H_3 (C_3D_3) radical formed via two-photon dissociation of benzene. The observed laser flux dependences of MPI efficiency and intensities of several major ions were analyzed with the rate equation model derived from the proposed scheme. As a result, more than 80% of the observed $C_3D_3^{+}$ ions were found to be produced from the C_3D_3 radical. The analyses also suggest the existence of at least two isomeric species for the C_3D_3 (C_3H_3) radical and the $C_4D_4^{+\cdot}$ ($C_4H_4^{+\cdot}$) ions, respectively.

Laser-multiphoton processes of benzene via the second singlet excited state, S_2 ($^1B_{1u}$), at 193 nm differ from those via the low vibrational states of the lowest singlet excited state, S_1 ($^1B_{2u}$), at the wavelengths longer than 248 nm. The following experimental results can characterize the two different processes. The first is that the lifetime of the S_2 state is very short.[1—4] This causes a remarkable decrease of the MPI efficiency at 193 nm.[5] The second is a different fragmentation behavior observed in the three-photon process. In the case of the S_1 excitation, the fragmentation occurs from the metastable ion having a total energy of 14—15 eV. On the other hand, in the case of the S_2 excitation, the excited molecular ion has a total energy of about 18 eV. Therefore, the distribution of the fragment ions and also the rate of the unimolecular dissociation are considerably different from each other.[6—10] The third is that "hot" benzene, i.e., highly vibrationally excited benzene in the ground electronic state, formed via internal conversion from the S_2 state[11] can produce a lot of neutral fragments under the collision-free condition.[12] Lee and his co-workers suggested that those neutral fragments could substantially contribute to the MPI process at 193 nm.[12] Recently we also provided some experimental evidences suggesting their important roles in the MPI of benzene at 193 nm: A significant enhancement of the MPI efficiency at high laser power and an unusually large relative intensity of $C_3D_3^{+}/C_4D_4^{+\cdot}$.[5] Furthermore, Reilly and his co-workers observed a very narrow peak in the MPI-photoelectron spectra of benzene at 193 nm.[3] They assigned this peak to the photoelectron emitted from the resonance-enhanced two-photon ionization of the excited carbon atom, C(^{1}D). It indicates that the carbon atom is formed in the multiphoton process of benzene at 193 nm. Highly efficient production of neutral carbon atoms is also known in the multiphoton processes of several aromatic molecules with visible-UV lasers.[13,14] However, the dominant precursor of any fragment ions formed via the S_1 state of benzene is the molecular ion, not the neutral fragments.[15]

As mentioned above, the MPI and fragmentation process of benzene via the S_2 state is so complicated that the scheme proposed for the MPI process via the S_1 state[16,17] is insufficient for this description.[5] In this work, we propose a new MPI and fragmentation scheme of benzene at 193 nm. The scheme is essentially based on the ladder switching model[16] but explicitly involves formation of the "hot" benzene and additional ionization processes of the neutral fragments such as C_3H_3. The observed laser flux dependences of the intensities of the major ions as well as the MPI efficiency are analyzed according to the proposed scheme with the rate equation model.

Experimental

MPI mass spectra (MPI MS) of benzene were observed by using the molecular beam apparatus coupled with a quadrupole mass filter reported previously.[18] The molecular beam of benzene was produced by expanding pure benzene gas at ca. 4 kPa. The pressure in the detection chamber ($\leq 6\times10^{-5}$ Pa) was low enough to neglect ion-molecule reactions in the ionizer. No trace of benzene dimer was detected under this condition. An excimer laser (ArF (193 nm) or KrF (248 nm), Lambda Physics EMG 102) crossed by the benzene beam was focused at the center of the ionizer of the quadrupole mass spectrometer. The spot area was $(0.55—1.1)\times10^{-2}$ cm^2 depending on the aperture size used. The laser flux, I (photons·cm^{-2}·s^{-1}), was evaluated by using the spot area, half-width of the laser pulse (15 ns) and the laser energy measured with a joule meter (ED 100A or ED 200 from Gentec Inc.). The ion signals were amplified with an electron multiplier and a preamplifier and averaged with a Boxcar averager in the time of flight mode. The sensitiv-

ity of the observed ion signal depending on the mass number was corrected with the method described previously.[19]

The MPI efficiency of gaseous benzene was measured with the method reported previously.[5,20] The ion pulse was observed with a digital oscilloscope at every laser shot. The volume of the ionization region was measured to be 0.018 $cm^2 \times 2.45$ cm under the unfocusing condition (ArF and KrF lasers) and 0.0031 $cm^2 \times 2.45$ cm under the weakly focusing condition (ArF laser), respectively. The pressure of gaseous benzene was varied from 0.7 to 4.0 Pa and from 0.7 to 1.3 Pa in the cases of ArF and KrF lasers, respectively. The integrated ion signals were found to increase linearly with increase of the pressure.

A set of linear differential equations presenting the rate equations derived from the proposed MPI scheme was analytically solved with the matrix method.[21] A brief description on its general solution is given in Appendix. The parameters involved were determined with the usual nonlinear least-squares fitting methods.[22,23]

Results and Analysis

MPI MS Data Used for Analysis. Figure 1 shows the laser flux dependences of the major fragment ions and the molecular ion observed in the MPI of benzene-d_6 at 193 nm. In Fig. 1, the sum of the intensities of $C_n^{+\cdot}$ ions (n=1,2,3) is found to amount to >95% of the total ion intensity at the highest laser flux (1.5×10^{26} photons·cm^{-2}·s^{-1}) at 193 nm. On the other hand, relative intensities of the other ions extremely decrease, e.g., the intensity of the $C_6D_6^{+\cdot}$ ion is only 0.10—0.15% of the total ion intensity. These trends in the distribution of the molecular and fragment ions have previously been reported.[1,3] From the exponents of the laser flux dependences the observed ions can be classified into either group of ions produced via two- or three- or higher than four-photon process, which are abbreviated to $2h\nu$ ions, $3h\nu$ ions and $\geq 4h\nu$ ions, respectively. This classification was found to be compatible with the data of appearance energies.[24,25] The $3h\nu$ ions at 193 nm contain five fragment ions: $C_3D_3^+$, $C_4D_4^{+\cdot}$, $C_4D_3^+$, $C_4D_2^{+\cdot}$, and $C_2D_3^+$. The latter three ions are formed via four-photon processes in the MPI at 248 nm, whereas both $C_6D_5^+$ and $C_6D_4^{+\cdot}$ ions, ones of the major $3h\nu$ ions at 248 nm, were undetectable at 193 nm under our experimental conditions in agreement with the previous observation.[1] The intensities of $3h\nu$, $\geq 4h\nu$ and total ions at a given laser flux were obtained by summing up the interpolated intensities of the relevant ions from the curves drawn in Fig. 1.

MPI and Fragmentation Scheme. We analyzed the laser flux dependences of MPI efficiencies of gaseous benzene and benzene-d_6 at 193 nm according to the usual simple four-state model given in Scheme 1. In this scheme all the ions are produced via the MPI processes of the molecular ion ($C_6H_6^{+\cdot}$ or $C_6D_6^{+\cdot}$). The observed dependences were reproducible only when the value of γ_{1S} is assumed to be smaller than 1×10^8 s^{-1}. This value, however, is much smaller than the acceptable one, i.e., $\geq 5 \times 10^{10}$ s^{-1}.[1—4] On the other hand, it was impossible to fit the data in the whole range of the laser flux investigated with any acceptable values of γ_{1S}, i.e., a significant enhancement of the MPI efficiency was observed at high laser fluxes. We have suggested the existence of an additional MPI process other than the fragmentation process via the molecular ion. As one of the most probable processes we can add the ionization of the neutral fragments formed via one-or two-photon dissociation of benzene. Those neutral fragments are known to be produced from "hot" benzene ([H]) as follows:[12]

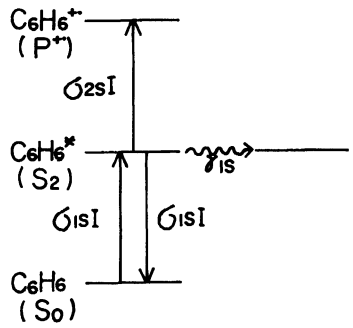

Scheme 1. Four-state MPI model.

$$[S_0] + h\nu \rightarrow [S_2] \rightarrow [H] \rightarrow C_6H_5, C_6H_4, C_5H_3 \quad \text{(R1)}$$

$$[H] + h\nu \rightarrow [H^*] \rightarrow C_3H_3 + C_3H_3 \quad \text{(R2)}$$

$$C_6H_5 + h\nu \rightarrow C_6H_4 + H, \quad \text{or} \quad C_4H_3 + H_2 \quad \text{(R3)}$$

The ionization of some benzene valence isomers such as fulvene, known as one of the major photoproducts of benzene, seems to be neglected in the laser pulse duration because its formation very slowly occurs.[11] From the following experimental results (i)—(iii) and the energetic consideration (iv), we propose that the C_3H_3 radical formed via the reaction Eq. R2 is the most probable radical species contributing to the additional MPI process.

(i) The enhancement of the MPI efficiency mentioned above occurs above the laser fluxes where the intensity of the $C_3D_3^+$ ion is comparable to that of the $C_6D_6^{+\cdot}$ ion.

(ii) The intensities of $C_6D_5^+$ and/or $C_6D_4^{+\cdot}$ ions are extremely weak or undetectable.

(iii) The relative intensity of $(C_4D_4^{+\cdot} + C_4D_3^+ + C_4D_2^{+\cdot})/C_3D_3^+$ is found to be 1—2 in the range of the observed laser fluxes in Fig. 1. This ratio is much smaller than the value of 3—5 estimated from the breakdown diagram of benzene.[6,7] The existence of an additional formation process of $C_3D_3^+$ ion is suggested.

(iv) The ionization of the C_3D_3 radical formed via the reaction Eq. R2 is likely to occur with only one-photon absorption, i.e., three-photon ionization in the overall process. In the reaction, the excited hot benzene [H*] could produce several isomers of C_3D_3 rad-

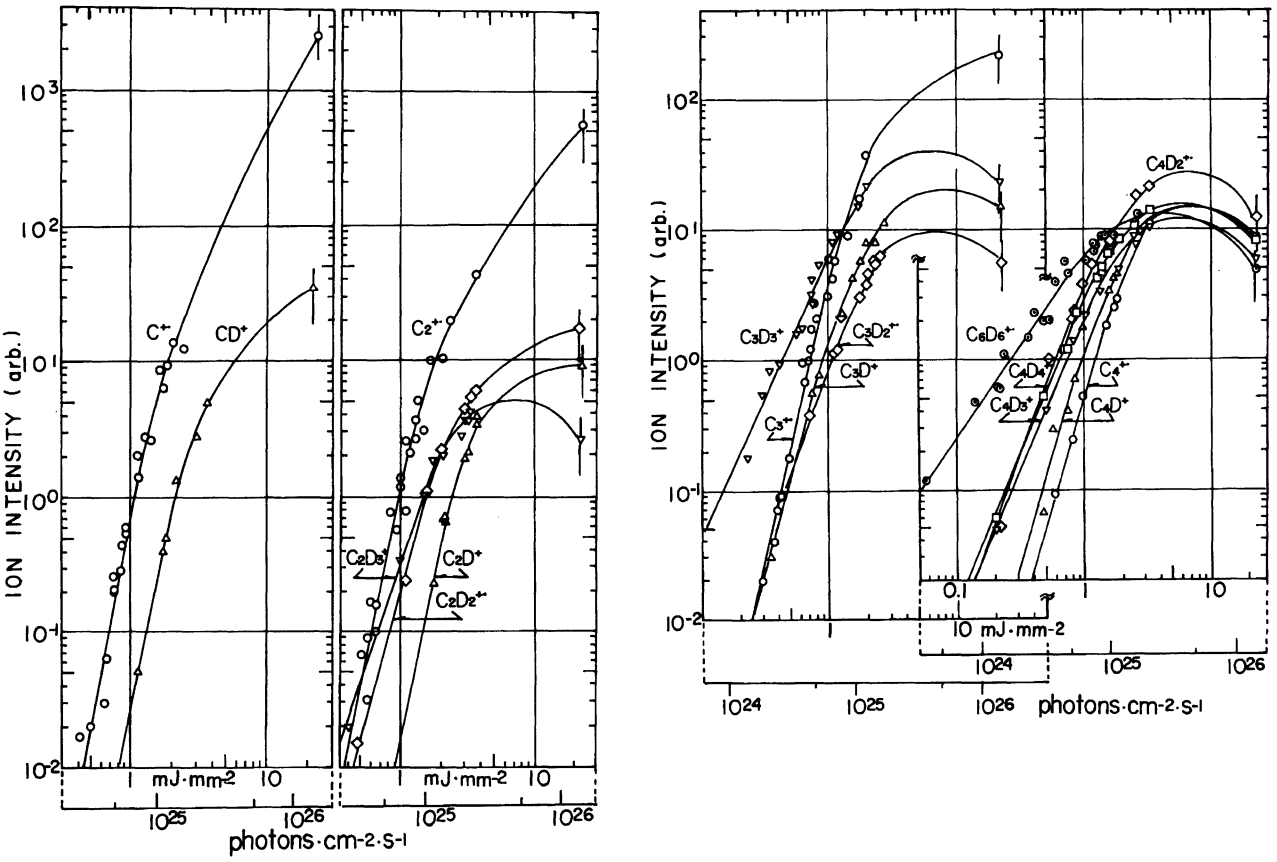

Fig. 1. Laser flux dependences of the intensities of ions produced in the MPI of benzene-d_6 at 193 nm: The intensity data at the highest laser flux (1.5×10^{26} photons·cm^{-2}·s^{-1}) were estimated from the observed relative intensities and the assumed total ion intensity (3500) since the measurements at this laser flux were carried out under the different conditions. The total ion intensity (3500) was estimated by extrapolating the intensity data obtained in the range of the laser fluxes below 3×10^{25} photons·cm^{-2}·s^{-1}. The errors were mainly due to the error of the estimated total ion intensity (±1000). The ion intensities observed below 3×10^{25} photons·cm^{-2}·s^{-1} involve the errors of 10—30% for most of the major ions while the errors for the higher-order fragment ions such as $C_n^{+\cdot}$ ions are considerably large ($\lesssim$100%) at low laser fluxes.

icals such as cyclopropenyl (CP) and propargyl (PG) radicals. As shown in Fig. 2, the PG radical is more stable than the CP radical, whereas the ionic species, PG^+, is less stable than the CP^+ ion. This diagram also shows that these two isomers of the C_3H_3 (C_3D_3) radical can energetically be ionized with one-photon absorption at 193 nm. However, the PG radical produced from the [H*] should have a very large excess energy of about 2.7 eV. If this excess energy is stored mainly as the vibrational energy, leading to the formation of "hot" PG radical, one-photon ionization of the PG radical seems to hardly occur because of the very small Franck–Condon factors. On the other hand, the CP radical has a relatively small excess energy and also its ionization energy is low. Therefore, the CP radical could be ionized with one-photon absorption.

The MPI an fragmentation process of benzene at 193 nm becomes more complicated because the S_2 state very rapidly converts to the other states. The lifetime of the S_2 state is estimated to be 20 ps,[1] or probably much shorter.[2—4] Nakashima and Yoshihara reported that the S_2 state internally converts to the S_0 state (hot benzene) with a high yield (ca. 1).[11] Therefore, we must determine which state can effectively contribute to the formation of the molecular ion, the S_2 state, or the hot benzene ([H]) or the intermediate states ([X]) including highly vibrationally excited S_1 and triplet states (T_1, T_2, T_3). Thus the following four ionization processes are considered:

$$[S_0] + h\nu \rightarrow [S_2], \quad [S_2] + h\nu \rightarrow C_6D_6^{+\cdot} \qquad \text{(R4)}$$

$$[S_0] + h\nu \rightarrow [S_2] \rightarrow [X], \quad [X] + h\nu \rightarrow C_6D_6^{+\cdot} \qquad \text{(R5)}$$

$$[S_0] + h\nu \rightarrow [S_2] \rightarrow [H](\text{or } [X] \rightarrow [H]),$$
$$[H] + h\nu \rightarrow [H^*] \rightarrow 2C_3D_3, C_3D_3 + h\nu \rightarrow C_3D_3^+ \qquad \text{(R6)}$$

$$[S_0] + h\nu \rightarrow [S_2] \rightarrow [H](\text{or } [X] \rightarrow [H]),$$
$$[H] + h\nu \rightarrow C_6D_6^{+\cdot} \qquad \text{(R7)}$$

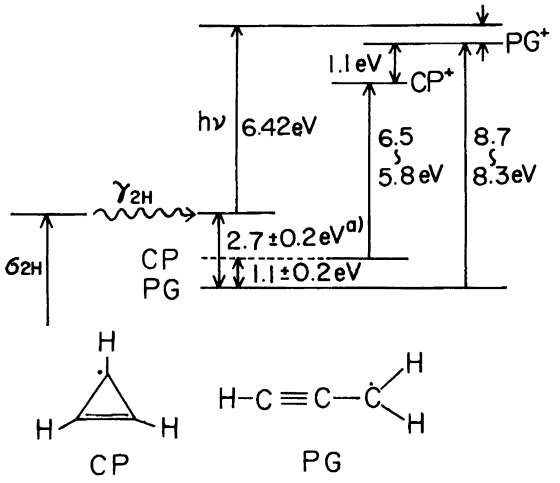

Fig. 2. Energy diagram related to the ionization of the two isomers (PG an CP) of C_3H_3 radicals: a) The released kinetic energy of 0.6 eV associated with the formation of C_3H_3 radical via two-photon dissociation is taken into account.[12] The following data of heats of formation (ΔH°_f) and ionization energies (IE) were used: ΔH°_f (C_6H_6)=0.86 eV,[26] ΔH°_f (CP)=4.55±0.17 eV,[27] ΔH°_f (PG)=3.5±0.2 eV,[12,28,29] IE (CP^+)=5.8[29]—6.5 eV,[27,30] IE (PG^+)=8.34[29]—8.68 eV.[30]

However, the process (Eq. R7), i.e., two-photon ionization via hot benzene, can be neglected because of the very small Franck–Condon factors associated with this ionization transition.[2,3] On the basis of these considerations, Scheme 2 is proposed for the MPI and fragmentation process of benzene at 193 nm.

MPI Efficiency and Total Ion Intensity. The MPI efficiency data at 193 nm were reanalyzed according to Scheme 2 involving the three ionization processes, (Eq. R4)—(Eq. R6). The fitting function for calculation of the ionization efficiency as a function of laser flux contains at least thirteen parameters: σ_{1S}, σ_{2S}, σ_{2X}, σ_{2H}, σ_{3H}, σ_{1NB}, γ_{1S}, γ_{XH}, γ_{1H}, γ_{2H}, γ_{0B}, ASX and α_{2HNB}. Among these parameters, the experimental values are available only for σ_{1S}. Those are given in Table 1. At this stage, we can reasonably assume that the value of σ_{2H} for benzene-d_6 is equal to 15 Mb, estimated value for benzene.[11] The orders of magnitudes of γ_{1S}, γ_{1H}, and γ_{2H} can also be estimated from the literature values to be $\geq 5\times10^{10}$ s^{-1},[1—4] 10^7 s^{-1},[12] and 10^7 s^{-1},[12] respectively. The other eight parameters, however, remain unknown. We tried to obtain the best fit values of σ_{2X} (or σ_{2S}) and σ_{1NB} for a given set of the following eight parameters: γ_{1S} (10^9, 10^{10}, 10^{11}, 10^{12}), ASX (1, 0.1, 0.05, 0.01, 0), γ_{XH} (10^7—10^9), γ_{1H} (10^6, 10^7, 5×10^7), γ_{2H} (10^6, 10^7, 5×10^7), γ_{0B} (0, 10^7, 10^8, 10^9, 10^{10}), $\sigma_{3H}=0$ and $\alpha_{2HNB}=1$. However, those parameters were not uniquely determined in this fitting procedure because the observed MPI efficiencies were well fitted with any set of the parameters. Curves 1 and 2 in Fig. 3, for instance, show the calculated MPI efficiencies of benzene-d_6 and benzene, respectively, where the best fit values of σ_{2X} and σ_{1NB} were determined by assuming that $\gamma_{1S}=1\times10^{11}$ s^{-1}, ASX=0.05, $\gamma_{XH}=1\times10^8$ s^{-1}, $\gamma_{1H}=1\times10^7$ s^{-1}, $\gamma_{2H}=1\times10^7$ s^{-1}, $\gamma_{0B}=1\times10^9$ s^{-1}, and $\sigma_{2S}=0$ Mb. The reliabilities of these values will be discussed later. Curve 1′ represents the MPI efficiency ascribable to the process Eq. R5 for benzene-d_6, calculated by assuming that $\sigma_{1NB}=0$. A significant deviation of the Curve 1 from the Curve 1′ is found to occur above the laser flux ($(3—5)\times10^{24}$ photons·cm^{-2}·s^{-1}) where the $3h\nu$ ions are abundantly formed (see Curve 4). The large deviation at high laser fluxes little depends on the assumed values of the parameters when $\gamma_{1S}\geq1\times10^9$ s^{-1}. It means that the ionization of the C_3D_3 radical (process Eq. R6) greatly contributes to the MPI efficiency. As shown in Curves 3 and 3′, similar deviation is also found for the dependences of the total ion intensities.

$C_6D_6^{+\cdot}$ Ion. We next tried to reduce the ambiguities of the parameters mentioned above by analyzing the laser flux dependence of $C_6D_6^{+\cdot}$ ion. Curves 6 and 7 in Fig. 4 were calculated as a function of γ_{1S} by assuming that the $C_6D_6^{+\cdot}$ ion is formed only via the S_2

Table 1. Absorption Cross Section, σ_{1S}, of Benzene at 193 nm

	C_6H_6		C_6D_6
σ_{1S}/Mb[a]	8.60±0.38[b]	(8.06±0.25)[c]	9.12±0.40[b]

a) Mb=10^{-18} cm^2. b) Ref. 5. c) Ref. 11.

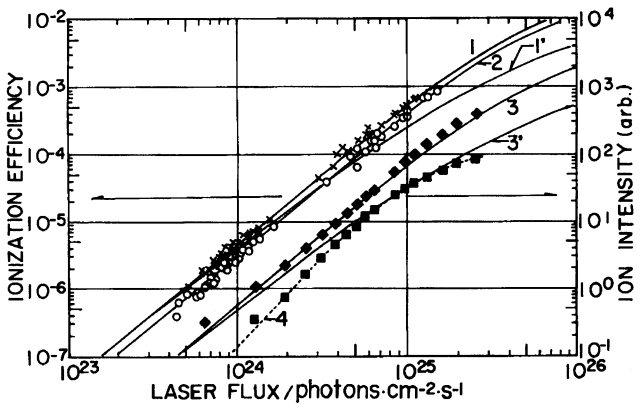

Fig. 3. Laser flux dependences of MPI efficiencies of benzene (○) and benzene-d_6 (×) and intensities of total ion (◆) and $3h\nu$ ions (■) in the MPI MS of benzene-d_6 at 193 nm: Curves 1—3 show the dependences calculated by assuming that $\gamma_{1S}=10^{11}$ s^{-1}, ASX=0.05 and $\gamma_{0B}=10^9$ s^{-1}. The following best fit values are used: C_6D_6 (Curves 1 and 3), $\sigma_{1S}=9.12$ Mb, $\sigma_{2X}=0.12$ Mb, and $\sigma_{1NB}=1.0$ Mb; C_6H_6 (Curve 2), $\sigma_{1S}=8.60$ Mb, $\sigma_{2X}=0.085$ Mb, and $\sigma_{1NB}=0.90$ Mb. Curves 1′ and 3′ show the dependences including no contribution of the ionization process Eq. R6. The dotted Curve 4 shows the experimental laser flux dependence of the intensity of the $3h\nu$ ions.

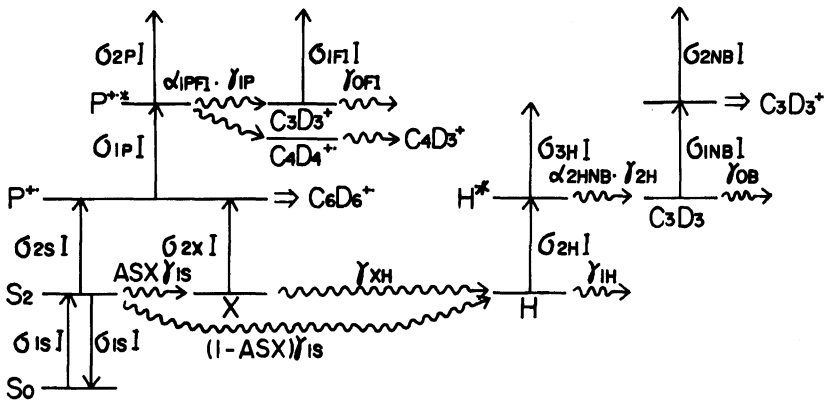

Scheme 2. MPI and fragmentation process of benzene at 193 nm.

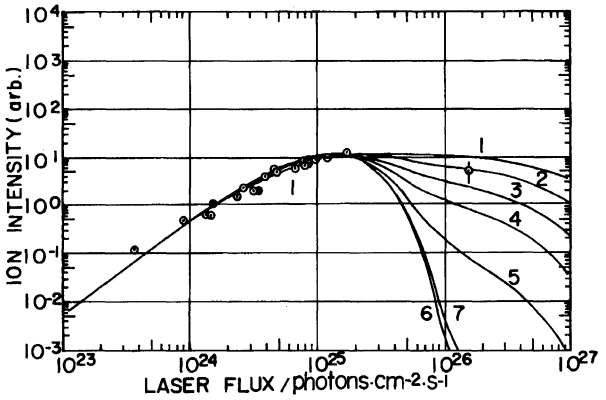

Fig. 4. Laser flux dependences of $C_6D_6^{+\bullet}$ ion at 193 nm: Curves 1—5 represent the dependences calculated as a function of γ_{XH} by assuming that ASX=0.05, $\gamma_{1S}=10^{11}$ s^{-1} and $\sigma_{2S}=0$. The best fit values of σ_{2X} and σ_{1P} were obtained for each of the assumed values of γ_{XH} as follows: Curve 1, $\gamma_{XH}=1\times10^{7}$ s^{-1}, $\sigma_{2X}=0.084$ Mb, $\sigma_{1P}=40$ Mb ; Curve 2, 1×10^{8}, 0.12, 26; Curve 3, 2×10^{8}, 0.17, 21 ; Curve 4, 3×10^{8}, 0.23, 18 ; Curve 5, 5×10^{8}, 0.34, 15. Curves 6 and 7 show the dependences calculated by assuming that ASX=0 and $\gamma_{1S}=10^{12}$ s^{-1} (Curve 6) or 10^{10} s^{-1} (Curve 7) where the following best fit values are used: $\sigma_{2S}=30$ Mb and $\sigma_{1P}=12$ Mb for Curve 6 and $\sigma_{2S}=0.30$ Mb and $\sigma_{1P}=12$ Mb for Curve 7.

state (process Eq. R4), i.e., ASX=0. The sudden fall-off of the $C_6D_6^{+\bullet}$ ion at the laser fluxes higher than 2×10^{25} photons·cm^{-2}·s^{-1} is in disagreement with the experimental data. As another extreme case, we consider the case where the $C_6D_6^{+\bullet}$ ion is formed only via the [X] state (process Eq. R5), i.e., $\sigma_{2S}=0$. The results are shown in Curves 1—5, calculated as a function of γ_{XH} in the range from 1×10^{7} to 5×10^{8} s^{-1} by assuming that ASX=0.05 and $\gamma_{1S}=10^{11}$ s^{-1}. The observed dependence is sufficiently reproduced by the Curve 2 drawn with the following parameters: $\gamma_{XH}=1\times10^{8}$ s^{-1}, $\sigma_{2X}=0.12$ Mb and $\sigma_{1P}=26$ Mb. The best fit values of these three parameters are almost the same for the assumed value of γ_{1S} larger than 10^{10} s^{-1}, but depend on the value of ASX as given in Table 2. These results give

Table 2. The Best Fit Values of γ_{XH}, σ_{2X}, and σ_{1P} Obtained for Four Different Values of ASX

ASX	γ_{XH}/s^{-1}	σ_{2X}/Mb	σ_{1P}/Mb
0.01	10^{7}—10^{8}	0.42—0.62	34—25
0.05	1×10^{8}	0.12	26
0.1	2×10^{8}	0.086	21
1.0	2×10^{8}	0.009	21

an evidence that the intermediate state [X] plays a very important role in the formation of benzene cation. The relative contribution of the two ionization processes via the [X] state and the S_2 state could not be estimated in these fitting procedures. The latter process, however, seems to be less important since the photoelectron peak corresponding to this process is rather minor.[3] So we roughly assume in the following fitting procedures that the benzene cation is formed only via the intermediate state [X], i.e., $\sigma_{2S}=0$. Some ambiguities may be caused by this assumption as follows: The best fit value of σ_{2X} was reduced from 0.12 to 0.08 Mb when the fitting was carried out by using an assumed value of σ_{2S}, for example, 1 Mb, which is smaller than the upper limit (3 Mb) estimated under the assumption: ASX=0 and $\gamma_{1S}=10^{11}$ s^{-1}.

From Table 2, the value of γ_{XH} is estimated to be $\leq10^{8}$ s^{-1}, almost independently of ASX. The relatively slow conversion suggests that the intermediate state is the triplet state(s) rather than the S_1 state internally converted with an excess energy of 1.7 eV. This is because such a highly vibrationally excited S_1 state is known to further convert to the S_0 state at a rate higher than 10^{10}—10^{11} s^{-1}.[31—34] The quantum yields for the intersystem crossing from the S_1 state to the lowest triplet state (T_1) of benzene have previously been obtained as a function of the excess energy less than 0.41 eV.[32] In this range the quantum yields are known to decrease with increase of the excess energy. At the largest excess energy investigated (0.41 eV) the yield was 0.29. With this yield the rate constant for the intersystem crossing has been estimated to be 2.9×10^{8} s^{-1},[32] or 10.6×10^{8} s^{-1}.[33] The excess energy of the S_1

state (1.7 eV) after the excitation at 193 nm is far beyond this range. Therefore the quantum yield is likely much smaller than 0.29. Indeed, the yield for the internal conversion from the S_2 state to hot benzene has been estimated to be ca. 1 (ASX=ca. 0) although a considerably large uncertainty is involved (±0.5).[11] From these data the value of ASX can reasonably be assumed to be ≤0.1. This can partially be supported by the trend that the fittings for some fragment ions such as $C_4D_4^{+\cdot}$ ion become poorer when ASX>0.1. When 0.01≤ASX≤0.1, the value of γ_{XH} is estimated to be 10^7—10^8 s^{-1}. This value is consistent with the value of $(2—5)\times10^7$ s^{-1} estimated by extrapolating the observed decay constants of the T_1 state to the excess energy of 2.8 eV.[31,32] A significant contribution of the triplet states (T_1 and possibly T_2) in the MPI of benzene at 193 nm has also been suggested by Reilly and his coworkers, based on the observed photoelectron spectra with ArF laser.[3]

At this stage, however, we can not more definitely determine the value of ASX. The following analyses of fragment ions were carried out by assuming that ASX= 0.05. The uncertainties of the parameters, therefore, have remained depending on the assumed value of ASX (≤0.1).

$C_4D_n^+$ (n=4,3,2) Ions and Isotope Effect. The laser flux dependences in Fig. 1 indicate that the $C_4D_3^+$ ion as well as the $C_4D_4^{+\cdot}$ ion is formed via three-photon processes and the relative intensity of $C_4D_4^{+\cdot}/C_4D_3^+$ is nearly constant (1.2) in the range of the laser fluxes investigated. Figure 1 also shows that the three-photon process in addition to higher order process, maybe four-photon process, considerably contributes to the formation of the $C_4D_2^{+\cdot}$ ion. These $3h\nu$ ions ($C_4D_n^+$; n=4,3,2) are considered to be produced mainly from the excited $C_6D_6^{+\cdot}$ ion formed via three-photon absorption. The excited $C_6D_6^{+\cdot}$ ion has a total energy of 18.4 (17.5) eV when the ionization occurs from the T_1 (T_2) state. This energy can exceed the appearance energies of the $C_4D_3^+$ and $C_4D_2^{+\cdot}$ ions (17.5 eV).[24] However, it is unlikely that these two fragment ions are formed directly from the excited $C_6D_6^{+\cdot}$ ion as is the $C_4D_4^{+\cdot}$ ion. This is because the observed isotope effects are very different among the $C_4D_n^+$ (n=4,3,2) ions. From Table 3, the intensity ratio of $C_4H_4^{+\cdot}/C_4D_4^{+\cdot}$ (0.65±0.11) measured under the same experimental conditions is found to be significantly smaller than the ratios of $C_6H_6^{+\cdot}/C_6D_6^{+\cdot}$ (0.88±0.06) and the other $3h\nu$ ions, i.e., $C_3H_3^+/C_3D_3^+$, $C_4H_3^+/C_4D_3^+$, and $C_4H_2^{+\cdot}/C_4D_2^{+\cdot}$. This trend is very different from the isotope effects observed at 248 nm, where all the ratios of $C_nH_m^+/C_nD_m^+$ for the major $3h\nu$ ions ($C_6H_5^+$, $C_6H_4^{+\cdot}$, $C_4H_4^{+\cdot}$, $C_3H_3^+$) are nearly equal to 1.3. Those large differences among the ratios of $C_4H_n^+/C_4D_n^+$ (n=4,3,2) result in the following intensity relations in the observed MPI MS at 193 nm: $C_4D_4^{+\cdot} > C_4D_3^+$ for benzene-d_6 and $C_4H_4^{+\cdot} < C_4H_3^+$ for benzene. The ratio of $(C_4H_4^{+\cdot}+C_4H_3^+ + C_4H_2^{+\cdot})/(C_4D_4^{+\cdot} + C_4D_3^+ + C_4D_2^{+\cdot})$, however, is about 0.9, which is nearly equal to the ratio of $C_6H_6^{+\cdot}/C_6D_6^{+\cdot}$. It is very likely that the $C_4D_3^+$ ion and some fraction of the $C_4D_2^{+\cdot}$ ion are produced from the $C_4D_4^{+\cdot}$ ion during its residence time in the ionizer.[35,36] In this case, the rate constant for the fragmentation should be at least larger than 1×10^5 s^{-1} judged from the residence time of the $C_4D_4^{+\cdot}$ ion (2—2.5 μs). On the other hand, such a labile $C_4D_4^{+\cdot}$ ion would completely be lost during its time of flight from the ionizer to the detector (46 μs). Nevertheless, the intensity of the $C_4D_4^{+\cdot}$ ion is comparable to that of the $C_4D_3^+$ ion. This result can be explained by supposing the existence of two kinds of $C_4D_4^{+\cdot}$ ions. One of them is rapidly decomposed in the ionizer yielding $C_4D_3^+$ and/or $C_4D_2^{+\cdot}$ ions and the other has a lifetime remaining during the time of flight. It is known that the $C_4H_4^{+\cdot}$ ion from benzene cation appears to be in two structural forms: 1-butene-3-yne (l-$C_4H_4^{+\cdot}$) and methylenecyclopropene (c-$C_4H_4^{+\cdot}$) cations.[9,10,37—42] Recent studies on the photodissociation of $C_4H_4^{+\cdot}$ ion made it clear that the l-$C_4H_4^{+\cdot}$ ion eliminates H atom or H_2 molecule under a visible light irradiation.[41,42] The relative intensity of the photoproducts, $C_4H_3^+/C_4H_2^{+\cdot}$, slightly increases from 1.5 obtained near the threshold energy (2.7—2.9 eV) with increase of the internal energy.[42] The reactive l-$C_4H_4^{+\cdot}$ ion is known to be by 0.2—0.5 eV less stable than the unreactive c-$C_4H_4^{+\cdot}$ ion.[9,40,43] Figure 5 shows the energetic diagram related to the formation and fragmentation of $C_4H_4^{+\cdot}$ ion. We propose that only the c-$C_4H_4^{+\cdot}$ ion is detectable as $C_4H_4^{+\cdot}$ ion while the l-$C_4H_4^{+\cdot}$ ion can completely decompose into $C_4H_3^+$ and $C_4H_2^{+\cdot}$ ions. The branching ratio is estimated to be 0.42 : 0.35 : 0.23 for c-$C_4D_4^{+\cdot}$: $C_4D_3^+$: $C_4D_2^{+\cdot}$ by using the data of $C_4D_3^+/C_4D_2^{+\cdot}$ (=1.5) and $C_4D_4^{+\cdot}/C_4D_3^+$ (=1.2). The resulting fraction of the l-$C_4D_4^{+\cdot}$ ion (=$C_4D_3^+ + C_4D_2^{+\cdot}$) is 0.58, which agrees with the literature values (>0.50) at total energy of $C_6H_6^{+\cdot}$ ion above 16.8 eV.[10]

This scheme for the formation of $C_4D_n^+$ ion (n=4,3,2) can reasonably explain the observed remarkable difference in the isotope effect for these ions. The most probable origin comes from the isotope effect attributable to the rate constant for the reaction: l-$C_4H_4^{+\cdot} \rightarrow C_4H_3^+ + H$. If the rate for this fragmenta-

Table 3. Isotope Effect on the Relative Intensity of $C_nH_m^+/C_nD_m^+$ in MPI of Benzene and Benzene-d_6 at 193 and 248 nm[a)]

	$C_6H_6^{+\cdot}$	$C_4H_4^{+\cdot}$	$C_4H_3^+$	$C_4H_2^{+\cdot}$	$C_3H_3^+$
193 nm	0.88±0.06	0.65±0.11	0.98±0.07	0.95±0.10	0.80±0.06
248 nm	1.18±0.05	1.33±0.06	1.1 ±0.1	1.1 ±0.1	1.28±0.06

a) The ratios were almost independent of the laser flux in the range from 2 to 10×10^{24} photons·cm^{-2}·s^{-1} at 193 nm and from 3.6 to 7.1×10^{25} photons·cm^{-2}·s^{-1}.

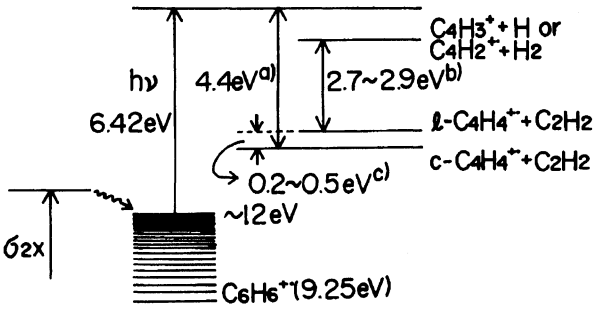

Fig. 5. Energy diagram for three-photon formation of $C_4H_n^+$ (n=4,3,2): a) The excess energy of c-$C_4H_4^{+\cdot}$ is evaluated by using the total energy of $C_6H_6^{+\cdot}$ (18.4 eV) and the appearance energy of $C_4H_4^{+\cdot}$ (14±0.2 eV).[24] b) Ref. 42. c) Refs. 9, 40, and 43.

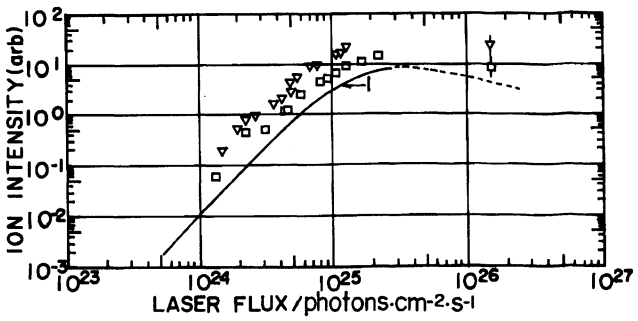

Fig. 6. Laser flux dependences of $C_3D_3^+$ (▽) and $C_4D_4^{+\cdot}$ (□) at 193 nm: Curve 1 shows the intensity of the $C_3D_3^+$ ion attributable to the process Eq. R8 (see text).

tion for the l-$C_4D_4^{+\cdot}$ ion is much slower than that for the l-$C_4H_4^{+\cdot}$ ion, some fraction of the l-$C_4D_4^{+\cdot}$ ions, especially having the excess energy near the threshold, may be detectable as $C_4D_4^{+\cdot}$ ion, leading to the increase of the intensity of $C_4D_4^{+\cdot}$ ion and the decrease of $C_4D_3^+$ and $C_4D_2^{+\cdot}$ ions.

Formation of $C_3D_3^+$ Ion. In Scheme 2, $C_3D_3^+$ ($C_3H_3^+$) ion is formed via two kinds of three-photon processes: one-photon ionization of the C_3D_3 (CP) radical (process Eq. R6) and the following direct fragmentation process from $C_6D_6^{+\cdot}$ ion:

$$[S_0] + 2h\nu \rightarrow C_6D_6^{+\cdot}, \quad C_6D_6^{+\cdot} + h\nu \rightarrow C_3D_3^+ \qquad \text{(R8)}$$

The branching ratio (α_{1PFI}) for the process Eq. R8 is estimated to be 0.2.[6,7] The excess energy of the $C_3D_3^+$ ion formed via the process Eq. R8 (<4.4 eV) is not enough to exceed the threshold energy (7 eV) for the elimination of D atom,[35] i.e., γ_{0FI}=0 in Scheme 2. The intensity of the $C_3D_3^+$ ion attributable to this process Eq. R8, is estimated to be in the order of 25% of sum of the $3h\nu$ $C_4D_n^+$ ions (n=4,3,2), i.e., about half of the $C_4D_4^{+\cdot}$ ion intensity. This contribution is only 10—20% of the observed intensity of the $C_3D_3^+$ ion as shown in Fig. 6. Therefore, most of the $C_3D_3^+$ ions (80—90%) are formed via the ionization of the C_3D_3 radical (process Eq. R6).

The laser flux dependence of the $C_3D_3^+$ ion could be analyzed according to Scheme 2. Here we neglected three-photon ionization via the [H*] species (σ_{3H}=0) and assumed that all the C_3D_3 radicals are primarily formed as the CP radical in the reaction Eq. R3 (α_{2HNB}=1). When $\gamma_{2H}=1\times10^7$ s^{-1}, the fitting was relatively poor at high laser fluxes for any values of γ_{0B} smaller than 1×10^8 s^{-1}. This trend was confirmed for any values of γ_{2H} in the range from 1×10^6 to 5×10^7 s^{-1} and of α_{2HNB} from 0.1 to 1.0 with a constant value of γ_{2H} (1×10^7 s^{-1}). The estimated values of σ_{1NB} and σ_{2NB} involve rather large ambiguities because these parameters strongly depend on γ_{0B}: (σ_{1NB}, σ_{2NB}, γ_{0B})= (1 Mb, 40 Mb, 1×10^9 s^{-1}) or (9 Mb, 30 Mb, 1×10^{10} s^{-1}). Although we could not estimate the upper limit of γ_{0B}, the C_3D_3 (CP) radical is likely to rapidly transform into its isomeric species or smaller neutral fragments. We assumed that $\gamma_{0B}=1\times10^9$ s^{-1} for calculation of the curves in Fig. 3.

Discussion

Formation of Neutral Fragments at 193 nm. The yield of C_6H_5 radical formed via one-photon process at 193 nm was calculated as a function of γ_{1H} according to Scheme 3, where the branching ratio (α_{1HNA}= 0.8) reported in Ref. 12 was used. The calculated yields of the C_6H_5 radical at the low laser flux of 5×10^{23} photons·cm^{-2}·s^{-1} were 0.17, 0.046, 0.023, and 0.0046 when $\gamma_{1H}=5\times10^7$, 1×10^7, 5×10^6, and 1×10^6 s^{-1}, respectively. At this laser flux the secondary photodissociation process Eq. R3 can be neglected. The yields for the C–H photodissociation of gaseous benzene are estimated to be 0.01 at 184.9 nm[44] and ≤0.02 at 193 nm.[11] The latter was obtained under the condition of benzene pressure where the collision number between benzene molecules is <1 during the laser irradiation (15 ns). Even if we consider very rapid collisional deactivation process of the hot benzene, the yield of 0.17, calculated with 5×10^7 s^{-1} for γ_{1H}, seems to be too large. The value of γ_{1H} (1×10^7 s^{-1}) used in our analysis is perhaps the upper limit. Figure 7 shows the laser flux dependences of the calculated yields of neutral fragments (NFs) and ions at 193 nm, where the following values were used: $\gamma_{1H}=1\times10^7$ s^{-1}, $\gamma_{2H}=1\times10^7$ s^{-1}, and σ_{1NA}=55 Mb.[12] Curve 2 shows the dependence of $1h\nu$ NFs (sum of C_6H_5, C_6H_4, and C_5H_3). The yield amounts to the maximum value of 0.3 at 5×10^{24} photons·cm^{-2}·s^{-1} (5 MW cm^{-2}). This saturation occurs almost independently of γ_{1H} in the range from 1×10^6 to 5×10^7 s^{-1}. Curve 5 gives the dependence of $2h\nu$ NF (C_3H_3). From this curve, it is found that the yield is extremely large (0.90) above the laser flux larger than 5×10^{25} photons·cm^{-2}·s^{-1}. The calculated ratio of $2h\nu$ NFs/$1h\nu$ NFs (Curve 5/Curve 2) at 5 MW cm^{-2}

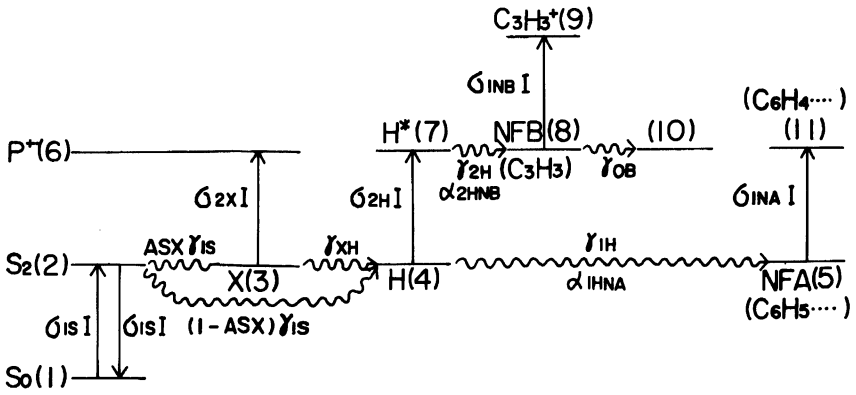

Scheme 3. Formation processes of neutral fragments and ions at 193 nm.

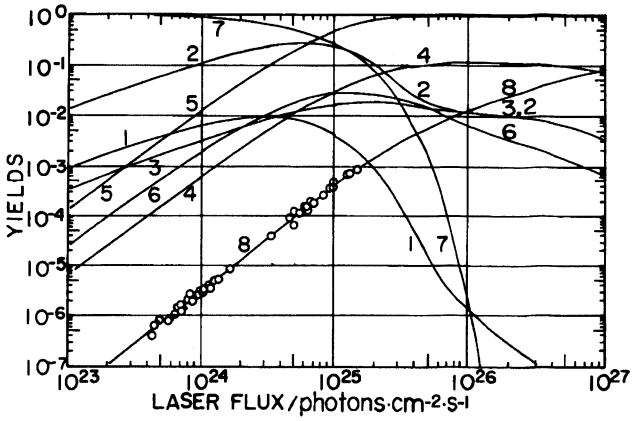

Fig. 7. Laser flux dependences of the yields of neutral fragments and ions formed via multiphoton process of benzene at 193 nm: Curves 1—8 show the dependences of the following neutral fragments and ions calculated according to Scheme 3: Curve 1, $1h\nu$ NFs detectable immediately after the laser irradiation (T=15 ns) (NFA(5)); Curve 2, sum of $1h\nu$ NFs ($S_2(2)$+X(3)+H(4)+NFA(5)); Curve 3, intermediate state (X(3)); Curve 4, $2h\nu$ NFs at T=15 ns (NFB-(8)+(10)); Curve 5, sum of $2h\nu$ NFs (H*(7)+NFB-(8)+(10)); Curve 6, $2h\nu$ NFs (secondary) ((11)); Curve 7, unexcited benzene molecule ($S_0(1)$); and Curve 8, ions ($P^{+\cdot}(6)=C_3H_3^+(9)$).

(0.5) was 2—3 times larger that the experimental value (0.2).[12] The yield of the secondary photodissociation product (Curve 6) is very low and becomes saturated around 1×10^{25} photons·cm^{-2}·s^{-1}.

Ionization of Neutral Fragments at 193 nm. At low laser flux the most abundant species formed via one-photon dissociation is known to be the C_6H_5 radical, which requires further two-photon absorption for its ionization.[24] Both yields of the C_6H_5 radical and of its one-photon-excited species amount to ca. 1% at 5×10^{24} photons·cm^{-2}·s^{-1} (see Curves 1 and 6 in Fig. 7). However, the $C_6H_5^+$ ion was an extremely minor ion. This means that the ionization cross section of the excited C_6H_5 radical is very small. In other words, the excited C_6H_5 radical rapidly decomposes into the secondary photodissociation products such as C_6H_4 species without ionization. In this process, "hot" C_6H_5 radical may be formed as hot benzene in one-photon excitation of benzene.

With increase of the laser flux, the $1h\nu$ NFs decrease while the $2h\nu$ NFs and the secondary photodissociation products increase. Since the $2h\nu$ NFs are abundantly produced during the laser irradiation, i.e., 10% at the laser flux larger than 5×10^{25} photons·cm^{-2}·s^{-1} (Curve 4 in Fig. 7), those $2h\nu$ NFs could have a chance of ionization at the high laser flux. The ionization is likely to occur directly via two-photon excitation of the $2h\nu$ NFs or via higher order ionization of the photodissociation products of the $2h\nu$ NFs. In the former two-photon ionization process, the fragment ions such as $C_3H_2^{+\cdot}$ and C_3H^+ is likely to be formed because the excess energy is sufficiently large. The latter process may contribute to the formation of the excited carbon atom C(^{1}D), known as one of the sources of the abundant $C^{+\cdot}$ ion in the MPI at 193 nm. From thermochemical aspect, the C(^{1}D) elimination reaction from the C_3H_3 radical seems to occur via at least one-photon excitation: $C_3H_3+h\nu\rightarrow C_2H_3$(vinyl)$+$C(^{1}D), where the following heats of formation are available: ΔH°_f (C(^{1}D))= 1.26 eV,[26] ΔH°_f (C_2H_3)=3.10 eV (vinyl radical)[27] and ΔH°_f (C_3H_3)=3.5 eV (PG radical),[12,28,29] 4.55 eV (CP radical).[27] If this reaction really occurs the $C^{+\cdot}$ ion could be formed via the following five-photon process: $[S_0]+h\nu\rightarrow[S_2]\rightarrow[H]$, $[H]+h\nu\rightarrow[H^*]\rightarrow C_3H_3$, $C_3H_3+h\nu\rightarrow C_2H_3+$C(^{1}D), C(^{1}D)$+2h\nu\rightarrow C^{+\cdot}$. Since the ionization process of C(^{1}D) involves the resonant absorption from ^{1}D to ^{1}P this process seems to effectively contribute to the formation of the $C^{+\cdot}$ ion at high laser flux.[3]

Summary

The MPI and fragmentation processes of benzene and benzene-d_6 via the S_2 state at 193 nm were investigated and compared with the processes via the S_1 state at 248 nm. The laser flux dependences of the MPI efficiencies and the MPI MS observed at 248 nm can be explained by the usual MPI scheme proposed previ-

ously. On the other hand, the dependences observed at 193 nm show several remarkable differences: (i) an unexpected enhancement of the MPI efficiency at high laser flux, (ii) an unusual isotope effect in the relative intensity of $C_4H_4^{+\bullet}/C_4D_4^{+\bullet}$, (iii) relatively abundant $C_3H_3^+$ ($C_3D_3^+$) ion, (iv) negligible or minor roles of $C_6H_5^+$, $C_6H_4^{+\bullet}$, and $C_6H_6^{+\bullet}$ ions, (v) similar laser flux dependences of $C_4H_4^{+\bullet}$ and $C_4H_3^+$ ions, and (vi) extremely abundant $C^{+\bullet}$, $C_2^{+\bullet}$, and $C_3^{+\bullet}$ ions at relatively low laser fluxes. Some of them, for example, (iv)—(vi), had previously been pointed out about ten years ago. However, their mechanistic descriptions were rather limited to the qualitative ones or two-photon ionization processes. This is because the processes involved are very complicated as mentioned before and the data available in those days had been deficient to construct a probable model for the analysis. Recent study on the photodissociation of benzene by Lee and his co-workers[12] has provided an effective clue to revisit this problem.[5] In this work we proposed a new scheme for the analysis of the MPI processes at 193 nm based on their results in combination with the recent development in the study of the highly vibrationally excited S_1 state of benzene molecule. The scheme involves one-photon ionization of the C_3H_3 (C_3D_3) radical formed via two-photon dissociation of benzene in addition to two-photon formation of the molecular ion via the intermediate triplet state(s), possibly T_1 and/or T_2. The observed laser flux dependences and fragment ion distributions were consistently explained according to this scheme. As one of the most important results, we emphasize that the ionization channel of the neutral fragment greatly contributes to the formation of the fragment ions. In particular, more than 80% of the $C_3H_3^+$ ($C_3D_3^+$) ions are formed via this process. Extremely high yield of the neutral fragments is likely to result in such anomalies observed in the MPI at 193 nm. The analyses also suggest that the isomeric species of C_3H_3 radical and $C_4H_4^{+\bullet}$ ion play an important role in the one-photon ionization of the C_3H_3 radical and the fragmentation of the excited $C_6H_6^{+\bullet}$ ion, respectively.

Several unknown parameters were estimated with the nonlinear least-squares fitting methods. Those will provide useful informations to understand the laser-induced multiphoton processes of benzene. However, some of them, especially the parameters related to the ionization of the neutral fragments, have inevitably large ambiguities because of the simplified MPI scheme proposed in this work and also many fitting parameters involved. More detailed investigations on the formation of the $2h\nu$ NFs and the detection of the neutral fragments such as $C(^1D)$ formed via higher order processes are necessary to define better the MPI and fragmentation process of benzene at 193 nm.

Appendix

Rate equations derived from Schemes 1, 2, and 3 are generally written by the following coupled set of linear differential equations:

$$dX(i,t)/dt = \sum_{j=1}^{L} A(i,j)X(j,t), \quad (1)$$

where the laser pulse having a rectangular temporal profile with a duration time of T is assumed. In this assumption, the rate constants associated with photoexcitation or stimulated emission are independent of time (t) in the range from 0 to T, which are approximately given by the corresponding absorption (or stimulated emission) cross section multiplied by the observed laser intensity in photons·cm^{-2}·s^{-1}. Chemical species in Schemes 1, 2, and 3 are numbered in such a way as a given species (i) except the ground state benzene ($i=1$) is produced from the low-numbered species (j, $j<i$). In this arrangement, all the values of $A(i,j)$ except $A(1,2)$ are equal to zero when $i<j$. The rate Eq. 1 can analytically be solved and the yield of the i-th species at time T, $X(i, T)$, is given by

$$X(i,T) = \sum_{j=1}^{L} C(j)P(i,j)\ \exp\ (\lambda(j)T), \quad (2)$$

where $\lambda(j)$, $P(i,j)$, and $C(j)$ are given by the following relations (i), (ii), and (iii), respectively.

(i) $\lambda(j)$ is the j-th eigen value of matrix A: $\lambda(1)$ or $\lambda(2)=(A(1,1)+A(2,2)+(D)^{1/2})/2$, $D=(A(1,1)-A(2,2))^2+4A(1,2)A(2,1)$, and $\lambda(j)=A(j,j)$ when $j>2$.

(ii) The elements of $P(i,j)$ are given as follows: $P(1,1)=A(1,2/(\lambda(1)-A(1,1))$, $P(1,2)=A(1,2)/(\lambda(2)-A(1,1))$, and $P(1,j)=0$ when $j>2$; $P(2,1)=1$, $P(2,2)=1$, and $P(2,j)=0$ when $j>2$; $P(i,i)=1$, $P(i,j)=0$ when $j>i$ and $i>2$, and

$$P(i,j) = \sum_{k=1}^{i-1} A(i,k)P(k,j)/(\lambda(j) - A(i,i))$$

for the other pairs of i and j ($i>j$).

(iii) The coefficient $C(i)$ can successively be determined by using the initial condition at time zero, i.e., X(i,0)=1 and $X(i,0)=0$ for the other species: $C(1)=A(2,1)/(\lambda(1)-\lambda(2))$, $C(2)=-C(1)$ and when $i>2$

$$C(i) = -\sum_{k=1}^{i-1} P(i,k)C(k).$$

The authors thank to Mr. Shinichi Shima, Mr. Tatemi Arichi, Mr. Akiyasu Yoneda, and Miss Miwako Kuniyasu for their assistance in the measurements of MPI MS. Thanks are also due to Dr. Hiroyuki Shinoda for helpful discussions.

References

1) J. P. Reilly and K. L. Kompa, *J. Chem. Phys.*, **73**, 5468 (1980).

2) H. Shinohara and N. Nishi, *Chem. Phys.*, **129**, 149 (1989); *J. Chem. Phys.*, **91**, 6743 (1989).

3) E. Sekreta, K. G. Owens, and J. P. Reilly, *Chem. Phys. Lett.*, **132**, 450 (1986).

4) F. Hirayama, T. A. Gregory, and S. J. Lipsky, *J. Chem. Phys.*, **58**, 4696 (1973).

5) Y. Mori, A. Yoneda, and T. Kitagawa, *Chem. Phys. Lett.*, **176**, 152 (1991).

6) J. H. D. Eland, R. Frey, H. Schulte, and B. Brehm, *Int. J. Mass Spectrom. Ion Phys.*, **21**, 209 (1976).
7) B. O. Jonsson and E. Lindholm, *Ark. Fys.*, **39**, 65 (1967).
8) T. Baer, G. D. Willett, D. Smith, and J. S. Phillips, *J. Chem. Phys.*, **70**, 4076 (1979).
9) H. M. Rosenstrock, J. Dannacher, and J. F. Liebman, *Radiat. Phys. Chem.*, **20**, 7 (1982).
10) M. F. Jarrold, W. Wagner-Redeker, A. J. Illies, N. J. Kirchner, and M. T. Bowers, *Int. J. Mass Spectrom. Ion Processes*, **58**, 63 (1984).
11) N. Nakashima and K. Yoshihara, *J. Chem. Phys.*, **79**, 2727 (1983).
12) A. Yokoyama, X. Zhao, E. J. Hinsta, R. E. Continetti, and Y. T. Lee, *J. Chem. Phys.*, **92**, 4222 (1990).
13) R. L. Whetten, K-J. Fu, R. S. Tapper, and E. R. Grant, *J. Phys. Chem.*, **87**, 1484 (1983).
14) A. Bolovinos, S. Spyrou, A. C. Cefalas, J. G. Philis, and P. Tsekeris, *J. Chem. Phys.*, **85**, 2335 (1986).
15) R. S. Pandolfi, D. A. Gobeli, and M. A. El-Sayed, *J. Phys. Chem.*, **85**, 1779 (1981).
16) E. W. Schlag and H. J. Neusser, *Acc. Chem. Res.*, **16**, 355 (1983).
17) U. Boesl, R. Weinkauf, K. Walter, C. Weickhardt, and E. W. Schlag, *J. Phys. Chem.*, **94**, 8567 (1990).
18) Y. Mori and T. Kitagawa, *Int. J. Mass Spectrom. Ion Processes*, **64**, 169 (1985).
19) Y. Mori and T. Kitagawa, *Chem. Phys. Lett.*, **128**, 383 (1986).
20) U. Boesl, H. J. Neusser, and E. W. Schlag, *Chem. Phys.*, **55**, 193 (1981).
21) G. J. Fisanick, T. S. Eichelberger, IV, B. A. Heath, and M. B. Robin, *J. Chem. Phys.*, **72**, 5571 (1980).
22) J. A. Nelder and R. Meed, *Comput. J.*, **7**, 308 (1965).
23) P. R. Bevington, "Data Reduction and Error Analysis for the Physical Sciences," McGraw-Hill, New York (1969).
24) H. M. Rosenstock, K. Draxl, B. W. Steiner, and J. T. Herron, *J. Phys. Chem. Ref. Data, Suppl. 1*, **1977**, 6; R. D. Levin and S. G. Lias, "Ionization Potential and Appearance Potential Measurements 1971—1981," "NSRDS-NBS 71," U. S. Department of Commerce, Washington, D. C., 1982.
25) V. S. Antonov, V. S. Letokhov, and A. N. Shibanov, *Appl. Phys.*, **22**, 293 (1980).
26) "CRC Handbook of Chemistry and Physics," ed by R. C. Weast, CRC Press Inc., Boca Ratin (1979).
27) D. J. DeFrees, R. T. McIver, Jr., and W. J. Hehre, *J. Am. Chem. Soc.*, **102**, 3334 (1980).
28) W. Tsang, *Int. J. Chem. Kinet.*, **2**, 23 (1970).
29) J. L. Franklin, J. D. Dillard, H. M. Rosenstock, Y. T. Herron, K. Draxl, and F. M. Field, "Ionization Potentials, Appearance Potentials, and Heats of Formation of Gaseous Positive Ions," "NSRDS-NBS 26," U. S. Department Commerce, Washington, D. C., 1969.
30) F. P. Lossing, *Can. J. Chem.*, **50**, 3973 (1972).
31) M. A. Duncan, T. G. Dietz, M. G. Liverman, and R. E. Smalley, *J. Phys. Chem.*, **85**, 7 (1981).
32) C. E. Otis, J. L. Knee, and P. M. Johnson, *J. Phys. Chem.*, **87**, 2232 (1983).
33) M. Sumitani, D. V. O'Connor, Y. Takagi, N. Nakashima, K. Kamogawa, Y. Udagawa, and K. Yoshihara, *Chem. Phys.*, **93**, 359 (1985); D. V. O'Connor, M. Sumitani, Y. Takagi, N. Nakashima, K. Kamogawa, Y. Udagawa and K. Yoshihara, *Chem. Phys.*, **93**, 373 (1985).
34) S. Kato, *J. Chem. Phys.*, **88**, 3045 (1988).
35) W. Dietz, H. J. Neusser, U. Boesl, E. W. Schlag, and S. H. Lin, *Chem. Phys.*, **66**, 105 (1982).
36) H. Kuhlewind, H. J. Neusser, and E. W. Schlag, *Int. J. Mass Spectrom. Ion Phys.*, **51**, 255 (1983).
37) P. Ausloos, *J. Am. Chem. Soc.*, **103**, 3931 (1981).
38) C. Lifshitz, D. Gibson, K. Levsen, and I. Dotan, *Int. J. Mass Spectrom. Ion Phys.*, **40**, 157 (1981).
39) W. Wagner-Redecker, A. J. Illies, P. R. Kemper, and M. T. Bower, *J. Am. Chem. Soc.*, **105**, 5719 (1983).
40) M-Y. Zhang, C. Wesdemiotis, M. Marchetti, P. O. Danis, J. C. Ray, Jr., B. K. Carpenter, and F. W. McLafferty, *J. Am. Chem. Soc.*, **111**, 8341 (1989); M-Y. Zhang, B. K. Carpenter, and F. W. McLafferty, *J. Am. Chem. Soc.*, **113**, 9499 (1991).
41) W. J. van der Hart, *Org. Mass Spectrom.*, **23**, 187 (1988).
42) R. E. Krailler and D. H. Russell, *Org. Mass Spectrom.*, **20**, 606 (1985).
43) S. W. Staley and T. D. Norden, *J. Am. Chem. Soc.*, **111**, 445 (1989).
44) J. K. Foote, M. H. Mallon, and J. N. Pitts, Jr., *J. Am. Chem. Soc.*, **88**, 3698 (1966); F. Mellows and S. Lipsky, *J. Phys. Chem.*, **70**, 4076 (1966).